BLIND DECONVOLUTION OF BACKSCATTERED ULTRASOUND USING SPARSE SENSOR ARRAYS

Tao He and Carlos E. Davila

Electrical Engineering Department, Southern Methodist University, Dallas, TX 75205

ABSTRACT

A method for blind deconvolution of ultrasound and other inverse-scattering problems is presented. The method can be applied to one, two or three dimensional backscattered data. This paper focuses on the one and two dimensional cases. The method is based on a subspace-based blind deconvolution algorithm. In the two dimensional case, the blind deconvolution produces an unknown linear mixture of the reflectivity profile. An entropy minimization algorithm is used to retrieve the reflectivity data from the mixture. This method improves the lateral and axial resolution compared to conventional ultrasound B-scans.

1. INTRODUCTION

A model of ultrasonic backscattering that is often used is based on a linear convolution [1]

$$r(t) = \iiint \frac{e^{-2\alpha s}}{z} g(x,y,z) s(x,y) p(t - \frac{2z}{c}) dx dy dz \tag{1}$$

where $s(x,y)$ is the lateral distribution of the transmitted ultrasound wave, c is the speed of sound through the tissue, α is the average attenuation constant of the tissue in the ultrasound propagation path, and $g(x,y,z)$ is the tissue reflectivity. The reflected signal for the one-dimensional problem is

$$r(t) = \int g(z) p(t - \frac{2z}{c}) dz \tag{2}$$

If $p(t)$ and $r(t)$ are known, the tissue reflectivity $g(z)$ can be identified by using deconvolution methods [2, 3, 4, 5]. In practice, $p(t)$ cannot be accurately measured, so most recent approaches for ultrasound deconvolution have been based on *blind* deconvolution, which does not require knowledge of the transmitted ultrasound pulse. This paper is organized as follows. A method for ultrasound deconvolution based on second-order statistics is described in Section 2. In Section 3, a method for entropy minimization of an unknown mixture is presented. This method is used to demix the outcome of a two-dimensional second-order blind deconvolution. Several simulations are given in Section 4. Section 5 concludes this paper.

2. SECOND-ORDER BLIND DECONVOLUTION

2.1. One Dimensional Case

Equation (2) can also be expressed as a standard discrete-time convolution:

$$\mathbf{r} = \mathbf{g} * \mathbf{p} + \mathbf{v} \tag{3}$$

where $\mathbf{g}$ is the tissue reflectivity to be estimated with length K, $\mathbf{p}$ is the transmitted pulse with length L, $\mathbf{r}$ is the received signal with length $N = K+L-1$ and $\mathbf{v}$ is the measurement error with length N. Furthermore, (3) can be rewritten in matrix form as $\mathbf{r} = \mathbf{G}\mathbf{p} + \mathbf{v}$, where

$$\mathbf{G} = \begin{bmatrix} g(0) & 0 & \cdots & 0 \\ g(1) & g(0) & \cdots & 0 \\ \vdots & \vdots & \ddots & \vdots \\ g(L-1) & g(L-2) & \cdots & g(0) \\ \vdots & \vdots & \ddots & \vdots \\ g(K-1) & g(K-2) & \cdots & g(K-L) \\ 0 & g(K-1) & \cdots & g(K-L+1) \\ \vdots & \vdots & \ddots & \vdots \\ 0 & 0 & \cdots & g(K-1) \end{bmatrix}$$

$$\mathbf{r} = [\, r(0) \quad \cdots \quad r(N-1) \,]^T.$$
$$\mathbf{p} = [\, p(0) \quad \cdots \quad p(L-1) \,]^T.$$
$$\mathbf{v} = [\, v(0) \quad \cdots \quad v(N-1) \,]^T.$$

Subspace methods can be used to estimate $\mathbf{g}$ as in [6, 7].

2.2. Two-Dimensional Case

We assume the transmitted pulse is confined to a two-dimensional space, which we can model as a $L \times L$ pixel array (other dimensions can be chosen as well). The measured signal can be expressed as:

$$\mathbf{r} = \mathscr{G} * \mathbf{P} + \mathbf{v} \tag{4}$$

where

$$\mathbf{r} = [\, r(0) \quad \cdots r(N-1) \,]^T, N = K + L - 1$$

$$\mathscr{G} = \begin{bmatrix} g(0,0) & \cdots & g(0, L-1) \\ \vdots & \ddots & \vdots \\ g(K-1, 0) & \cdots & g(K-1, L-1) \end{bmatrix}$$

$$\mathbf{P} = \begin{bmatrix} p(0,0) & \cdots & p(0,L-1) \\ \vdots & \ddots & \vdots \\ p(L-1,0) & \cdots & p(L-1,L-1) \end{bmatrix}$$
$$\mathbf{v} = [\, v(0) \quad \cdots \quad v(N-1)\,]^T, N = K+L-1$$

The elements in the backscattered received signal can be expressed as:

$$r(t) = \sum_{n=n_{min}}^{n_{max}} \sum_{m=0}^{L-1} p(n,m) g(t-n,m) + v(t) \tag{5}$$

where $n_{min} = \max(0, t-K)$, $n_{max} = \min(t, L-1)$, and $t = 0, \cdots, N-1$. This model more accurately accounts for lateral variations in both the reflectivity and the transmitted pulse. Note also it corresponds to a discrete-time version of (1) limited to two dimensions. This model can be seen to be equivalent to Jensen's model for ultrasound backscatter [8]. The transmitted ultrasound pulse matrix $\mathbf{P}$ represents the pulse-echo field in Jensen's model and can be rewritten as a vector $\mathbf{p}$ with dimension $L^2 \times 1$:

$$\mathbf{p} = [\, \mathbf{p}_1 \quad \cdots \quad \mathbf{p}_L \,]^T \tag{6}$$

where $\mathbf{p}_i = [\, p(0,i) \cdots p(L-1,i)\,]$. Therefore, (4) can be rewritten as

$$\begin{aligned} \mathbf{r} &= \mathfrak{G}\mathbf{p} + \mathbf{v} \\ &= [\, \mathfrak{G}_1 \quad \cdots \quad \mathfrak{G}_L \,]\mathbf{p} + \mathbf{v} \end{aligned} \tag{7}$$

where $\mathfrak{G}_i$ is a Toeplitz matrix having the same structure as $\mathbf{G}$ but formed by the ith column of $\mathscr{G}$. Equation (7) is similar to the one-dimensional problem. We assume $\mathbf{v}$ to be white noise with variance $\sigma_{\mathbf{v}}^2$ and the transmitted pulse $\mathbf{p}$ to be persistently exciting with full rank autocorrelation matrix $\mathbf{R_p} = E[\mathbf{p}\mathbf{p}^T]$. Hence, the autocorrelation matrix of $\mathbf{r}$ is expressed as

$$\mathbf{R_r} = \mathfrak{G}\mathbf{R_p}\mathfrak{G}^T + \sigma_{\mathbf{v}}^2 \mathbf{I}_N \tag{8}$$

The first term on right-hand side, $\mathfrak{G}\mathbf{R_p}\mathfrak{G}^T$, has rank L^2, so the rank of the nullspace of $\mathbf{R_r}$ is $(N-L^2)$. In practice, $\mathbf{R_r}$ can be estimated using the received signal vectors given by

$$\mathbf{r}_j = [\, r_j(0) \quad \cdots \quad r_j(N-1)\,]^T, j = 1, \cdots, M \tag{9}$$

as $\hat{\mathbf{R}}_{\mathbf{r}} = \frac{1}{M}\sum_{j=1}^{M} \mathbf{r}_j \mathbf{r}_j^T$. We define the noise subspace of $\mathfrak{G}\mathbf{R_p}\mathfrak{G}^T$ as the $N \times (N-L^2)$ matrix $\mathbf{V}_N$. The columns of $\mathfrak{G}$ span the L^2-dimensional signal subspace which is orthogonal to the noise subspace. Therefore, we have

$$\mathbf{V}_N^T \mathfrak{G} = \mathbf{O}_{(N-L^2)\times L^2} \tag{10}$$

Let

$$\mathbf{V}_{N,i} = \mathbf{V}_N(i : i+K-1, :), i = 1, 2, \cdots, L \tag{11}$$

be a $K \times (N-L^2)$ submatrix of $\mathbf{V}_N$. Then

$$\mathbf{V}_{N,i}^T \mathbf{g}_j = \mathbf{O}_{(N-L^2)}, i = 1, \cdots, L; j = 1, \cdots, L \tag{12}$$

where $\mathbf{g}_j = [\, g(0,j) \quad \cdots \quad g(K-1,j)\,]^T$. Then $\mathbf{g}_j$ can be estimated by solving the equations

$$\hat{\mathbf{V}}_{N,i}^T \hat{\mathbf{g}}_j \approx \mathbf{O}_{(N-L^2)}, i = 1, \cdots, L; j = 1, \cdots, L \tag{13}$$

where the $\hat{\mathbf{V}}_{N,i}$ are submatrices of the noise subspace eigenvector matrix $\hat{\mathbf{V}}_N$ derived from $\hat{\mathbf{R}}_{\mathbf{r}}$ and

$$\hat{\mathbf{g}}_j = [\, \hat{g}(0,j) \quad \cdots \quad \hat{g}(K-1,j)\,]^T \tag{14}$$

Let $\hat{\mathscr{G}} = [\, \hat{\mathbf{g}}_1 \quad \hat{\mathbf{g}}_2 \quad \cdots \quad \hat{\mathbf{g}}_L \,]$. One possibility is to set the columns of $\hat{\mathscr{G}}$ equal to the eigenvectors associated with the smallest L eigenvalues of

$$\mathbf{R_V} = \sum_{i=1}^{L} \hat{\mathbf{V}}_{N,i} \hat{\mathbf{V}}_{N,i}^T \tag{15}$$

However, there is no guarantee that $\hat{\mathscr{G}} = \mathscr{G}$. In fact, $\hat{\mathscr{G}}$ is a linear mixture of $\mathscr{G}$. Equation (13) implies that $\hat{\mathbf{V}}_{N,i}$ has an L-dimension nullspace. Therefore any solution of (13) will lie in that nullspace spanned by $\hat{\mathbf{g}}_1, \hat{\mathbf{g}}_2, \cdots \hat{\mathbf{g}}_L$. The algorithm described below can be used to obtain $\mathscr{G}$ by demixing $\hat{\mathscr{G}}$.

3. ENTROPY MINIMIZATION ALGORITHM

For the sake of the following discussion, it is assumed that the probability distribution of pixels in ultrasound images is approximately binary. Consider the following theorems for binary random variables: (The corresponding proofs can be derived from chapter 15 in [9])

Theorem 1 *Assume $\mathbf{X}_i, i = 1, 2, \cdots, N$ are N binary random variables. Then a linear combination $\mathbf{Y} = \sum_{i=1}^{N} a_i \mathbf{X}_i$ will have an entropy that is greater than the entropy of any of the $\mathbf{X}_i$. That is, $H(\mathbf{Y}) \geq H(\mathbf{X}_i), i = 1, 2, \cdots N$.*

Theorem 2 *Assume $\mathbf{X}$ is an image matrix with dimension $N \times M$. Each column in $\mathbf{X}$ is a realization of a binary random variable $X_i, i = 1, 2, \cdots, M$. Let $\mathbf{Z}$ be a linear mixture of $\mathbf{X}$, i.e., each column of $\mathbf{Z}$ is a linear combination of the columns of $\mathbf{X}$. If a vector $\mathbf{y}$ is formed by a linear combination of the columns of $\mathbf{Z}$, i.e., $\mathbf{y} = \mathbf{Za}$, where $\mathbf{a} = [\, a(0) \quad a(1) \quad \cdots \quad a(M-1)\,]^T$. Then the entropy of $\mathbf{y}$ has no more than M local minima and each local minimum of $\mathbf{Za}$ corresponds to a column of $\mathbf{X}$.*

These theorems make it possible to estimate the columns of a binary image given an image whose columns are a mixture of the binary image.

3.1. Entropy Estimator using Kernel-Shaped Histogram

Assume X is a random variable with continuous probability density function $f(x)$, then its differential entropy $h(X)$ is defined as $h(X) = -\int f(x)\log_2 f(x)dx$. If we divide the range of X into bins of width Δ and assume the density is continuous within the bins, it can be shown that we can use $H(X) + \log_2 \Delta$ to approximate $h(X)$ [10], where $H(X)$ is the discrete entropy of X. Assume a histogram contains L bins. Given a center c_n and a bin width Δ, we can define each bin of the histogram. The nth bin is defined to be the interval $[c_n - \frac{\Delta}{2}, c_n + \frac{\Delta}{2}), 1 \leq n \leq L$. For samples $X_1, \cdots, X_N$, we define M_n to be the number of X_j falling in the interval $[c_n - \frac{\Delta}{2}, c_n + \frac{\Delta}{2})$, then we have $M_n = \sum_{j=1}^{N} Q\left(\frac{X_j - c_n}{\sigma}\right)$, where $\sigma = \frac{\Delta}{2}$ and $Q(x)$ is the kernel function. Let $p_n = \frac{M_n}{\sum_{n=1}^{L} M_n}$, then the differential entropy is defined by

$$h(X) = -\sum_{n=1}^{L} p_n \log_2 p_n + \log_2 \Delta \tag{16}$$

3.2. Steepest Descent Algorithm

Each column in $\hat{\mathscr{G}}$ is mixture of the columns in the tissue reflectivity matrix $\mathscr{G}$. Assume the demixing vector is $\mathbf{w}$, the reconstructed signal is $\mathbf{y} = \hat{\mathscr{G}}\mathbf{w}$, where $\mathbf{w} = [\,w(0) \cdots w(L-1)\,]^T$ and $\mathbf{y} = [\,y(0) \cdots y(K-1)\,]^T$. The vector $\mathbf{y}$ will have minimum entropy if $\mathbf{w}$ is the optimal demixing vector $\mathbf{w}_{opt}$. In this case $\mathbf{y}$ will correspond to one of the columns of $\mathscr{G}$. Other columns of $\mathscr{G}$ will correspond to local minima in the entropy cost function. The cost function $J(\mathbf{w})$ used to minimize entropy is simply the entropy of $\mathbf{y}$ $J(\mathbf{w}) = -\sum_{n=1}^{L} p_n \ln p_n$, where L is the number of bins and N is the length of demixed signal. A Gaussian function is used as the kernel function Q. The new vector $\tilde{\mathbf{w}}$ is computed as $\tilde{\mathbf{w}} = \mathbf{w} - \mu\frac{\partial J(\mathbf{w})}{\partial \mathbf{w}}$, where $\frac{\partial J(\mathbf{w})}{\partial \mathbf{w}}$ is computed as:

$$\frac{\partial J}{\partial \mathbf{w}} = -\sum_{n=1}^{L}\left(\frac{\partial p_n}{\partial \mathbf{w}}\ln p_n + \frac{\partial p_n}{\partial \mathbf{w}}\right) \tag{17}$$

We have

$$\frac{\partial p_n}{\partial \mathbf{w}} = \left(\frac{\sum_{i=0}^{K-1}(q(\frac{\hat{\mathfrak{g}}_i\mathbf{w} - c_n}{\sigma})\frac{\hat{\mathfrak{g}}_i}{\sigma})}{T}\right) - \left(\frac{\sum_{i=0}^{K-1} Q(\frac{\hat{\mathfrak{g}}_i\mathbf{w} - c_n}{\sigma})}{T^2}\sum_{j=1}^{L}\sum_{i=0}^{K-1}\left(q\left(\frac{\hat{\mathfrak{g}}_i\mathbf{w} - c_j}{\sigma}\right)\frac{\hat{\mathfrak{g}}_i}{\sigma}\right)\right) \tag{18}$$

where $\hat{\mathfrak{g}}_i = [\,\hat{g}(i,0) \quad \cdots \quad \hat{g}(i,L-1)\,]$, σ equals the bin width, $q(x) = \frac{\partial Q(x)}{\partial x}$ and $T = \sum_{j=1}^{L}\sum_{i=0}^{K-1} Q\left(\frac{\hat{\mathfrak{g}}_i\mathbf{w} - c_j}{\sigma}\right)$.

Due to the high correlation between two adjacent columns in an image, we cannot deflate $\mathbf{w}_{n+1}$ from $\mathbf{w}_i (i = 1, \cdots, n)$. Here, $\mathbf{w}_i$ corresponds to the demixing vector, where i indexes the chronological order in which successive image columns are found. It is not difficult to consistently find the column corresponding to the global minimum entropy. It is however harder to converge to a column having a local minimum entropy. If we assume a demixing vector has been found, we can find a new demixing vector if the step size is small and if the initial estimate of the new vector is given by $\mathbf{w}_k^{(0)} = \bar{\mathbf{w}}_{k-1} + \mathbf{e}$, where $\bar{\mathbf{w}}_{k-1}$ is the previously identified demixing vector and $\mathbf{e}$ is a noise vector. Once all image columns are found a registration algorithm is applied to reconstruct the image. Columns are also scaled so that adjacent columns have suitably matching contrasts.

4. SIMULATIONS

A 300×16 synthetic image $\mathbf{G}$ was used to model the tissue reflectivity. In the first experiment, the transmitted pulse $\mathbf{P}$ was generated as a 16×16 random matrix. The received signal was a two-dimensional convolution of $\mathbf{G}$ and $\mathbf{P}$. The outcome of the two-dimensional blind deconvolution produced the mixed reflectivity matrix which was subsequently demixed using the minimum entropy method. Fig. 1 shows that the reconstructed $\mathbf{G}$ matches the original image quite closely. The second experiment used Jensen's Field II Matlab package to generate simulated backscattered ultrasound [11]. A realistic tissue phantom was generated by mapping each pixel in $\mathbf{G}$ to randomly located point scatterers in a 2×4.6 mm region. The amplitude of a given point scatterer was proportional to the corresponding pixel amplitude in $\mathbf{G}$. A 16-transducer array was created in the Field II program and was used as both the transmitter and receiver. The center frequency of each transducer was 5MHz and the sampling rate was 100MHz. To generate a random pulse-echo field, each transducer was excited by a statistically independent random pulse. The dimension of $\mathbf{P}$ was 16×16. A 16-line image was obtained using the backscattered data produced by Field II and the blind deconvolution/minimum entropy algorithm. The result is shown in Fig. 2. Since $\mathbf{P}$ is only an approximation to the real pulse-echo field, there is some visible distortion between the reconstructed image and the real image. A conventional B-scan was then obtained using the Field II program using the same 16-element array. The blind deconvolution image has considerably more resolution than the conventional B-scan (Fig. 2).

5. CONCLUSION

An algorithm for solving inverse scattering problems in ultrasound was described. This approach has the potential to improve on the resolution available using conventional linear arrays.

6. REFERENCES

[1] A. Macovski, *Medical Imaging Systems*, Prentice-Hall, 1983.

[2] M. Fatemi and A Kak, "Ultrasonic b-scan imaging: Theory of image formation and a technique for restoration," *Ultrasonic Imaging*, vol. 2, pp. 1–47, Jan. 1980.

[3] A. Herment, G. Demoment, and M. Vaysse, "Algorithm for on line deconvolution of echographic signals," *Acoustical Imaging*, vol. 10, pp. 325–345, 1980.

[4] W. Vollmann, "Resolution enhancement of ultrasonic b-scan images by deconvolution," *IEEE Trans. on Sonics Ultrason.*, vol. SU-29, pp. 78–83, March 1982.

[5] G. Demoment, R. Reynaud, and A. Herment, "Fast minimum variance deconvolution," in *Proc. Sixth Annual Conference of the IEEE Engineering in Medicine and Biology Society*, Los Angeles, Sept. 1984, p. 288.

[6] T. J. Endres, B. Anderson, J. C. R. Johnson, and L. Tong, "On the robustness of fir channel identification from fractionally spaced received signal second-order statistics," *IEEE Signal Processing Letters*, vol. 3, pp. 153–155, May 1996.

[7] A. P. Liavas, P. A. Regalia, and J. P. Delmas, "Robustness of least-squares and subspace methods for blind channel identification/equalization with respect to effective channel undermodeling/overmodeling," *IEEE Trans. on Signal Processing*, vol. 47, pp. 1636–1645, June 1999.

[8] J. A. Jensen, "A model for the propagation and scattering of ultrasound in tissue," *J. Acoust. Soc. Am.*, pp. 182–191, 1991.

[9] A. Papoulis, *Probability and Random Variables and Stochastic Processes*, McGraw-Hill, 3rd edition, 1991.

[10] T. M. Cover and J. A. Thomas, *Elements of Information Theory*, John Wiley & Sons, 1991.

[11] J. A. Jensen, "Field: A program for simulating ultrasound systems," *Medical & Biological Engineering & Computing*, vol. 34, pp. 351–353, 1996.

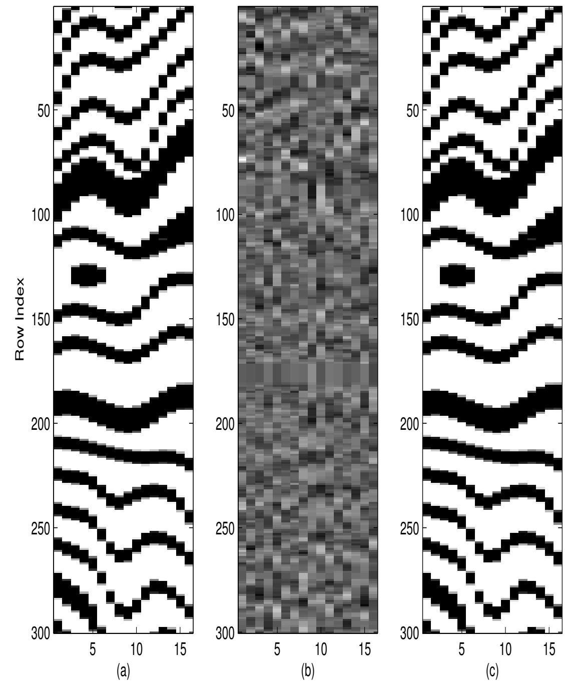

Fig. 1: Experiment 1.
(a) Original reflectivity; (b) Outcome of 2D Blind Deconvolution; (c) Reconstructed Image

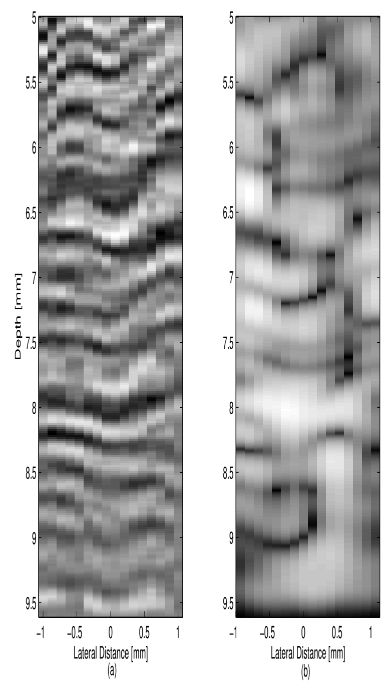

Fig. 2: Experiment 2.
Field II simulations: (a) Reconstructed Image using blind deconvolution/minimum entropy; (b) Conventional B-scan.